

# CD44 Variant 6 is Associated With Prostate Cancer Metastasis and Chemo-/Radioresistance

Jie Ni,<sup>1,2</sup> Paul J. Cozzi,<sup>2,3\*</sup> Jing L. Hao,<sup>1,2</sup> Julia Beretov,<sup>1,2,4</sup> Lei Chang,<sup>1,2</sup> Wei Duan,<sup>5</sup> Sarah Shigdar,<sup>5</sup> Warick J. Delprado,<sup>6</sup> Peter H. Graham,<sup>1,2</sup> Joseph Bucci,<sup>1,2</sup> John H. Kearsley,<sup>1,2</sup> and Yong Li<sup>1,2\*\*</sup>

<sup>1</sup>Cancer Care Centre and Prostate Cancer Institute, St George Hospital, Kogarah, Australia

<sup>2</sup>St George and Sutherland Clinical School, University of New South Wales (UNSW), Kensington, Australia

<sup>3</sup>Department of Surgery, St George Hospital, Kogarah, Australia

<sup>4</sup>SEALS, Anatomical Pathology, St George Hospital, Kogarah, Australia

<sup>5</sup>School of Medicine, Deakin University, Waurn Ponds, Australia

<sup>6</sup>Douglass Hanly Moir Pathology, Sydney, Australia

**INTRODUCTION.** Prostate cancer (CaP) is the second leading malignancy in older men in Western countries. The role of CD44 variant 6 (CD44v6) in CaP progression and therapeutic resistance is still uncertain. Here, we investigated the roles of CD44v6 in CaP metastasis and chemo/radioresistance. Expression of CD44v6 in metastatic CaP cell lines, human primary CaP tissues and lymph node metastases was assessed using immunofluorescence and immunohistochemistry, respectively.

**METHODS.** Knock down (KD) of CD44v6 was performed in PC-3M, DU145, and LNCaP cells using small interfering RNA (siRNA), and confirmed by confocal microscope, Western blot and quantitative real time polymerase chain reaction (qRT-PCR). Cell growth was evaluated by proliferation and colony formation assays. The adhesive ability and invasive potential were assessed using a hyaluronic acid (HA) adhesion and a matrigel chamber assay, respectively. Tumorigenesis potential and chemo-/radiosensitivity were measured by a sphere formation assay and a colony assay, respectively.

**RESULTS.** Over-expression of CD44v6 was found in primary CaP tissues and lymph node metastases including cancer cells and surrounding stromal cells. KD of CD44v6 suppressed CaP proliferative, invasive and adhesive abilities, reduced sphere formation, enhanced chemo-/radiosensitivity, and down-regulated epithelial-mesenchymal transition (EMT), PI3K/Akt/mTOR, and Wnt/ $\beta$ -catenin signaling pathway proteins in vitro.

**CONCLUSIONS.** Our findings demonstrate that CD44v6 is an important cancer stem cell-like marker associated with CaP proliferation, invasion, adhesion, metastasis, chemo-/radioresistance, and the induction of EMT as well as the activation PI3K/Akt/mTOR and Wnt signaling pathways, suggesting that CD44v6 is a novel therapeutic target to sensitize CaP cells to chemo/radiotherapy. *Prostate* 74:602–617, 2014. © 2014 Wiley Periodicals, Inc.

**KEY WORDS:** CD44 variant 6; prostate cancer; chemoresistance; radioresistance; PI3K/Akt/mTOR pathway; Wnt pathway

Grant sponsor: NH&MRC Career Development Fellowship; Grant sponsor: Surgical & Urological Research Fund (SURF) Urology Sydney; Grant sponsor: Cancer Research Trust Fund at Cancer Care Centre; Grant sponsor: Prostate and Breast Cancer Foundation.

The authors declare that they have no conflicts of interest.

\*Correspondence to: Associate Professor Paul Cozzi, MD, Department of Surgery, St George Hospital, Sydney, Australia.  
E-mail: pcozzi@unsw.edu.au

\*\*Correspondence to: Associate Professor Yong Li, MD, PhD, Cancer Care Centre, St George Hospital, Gray St Kogarah, Sydney, NSW 2217, Australia. E-mail: y.li@unsw.edu.au

Received 22 October 2013; Accepted 23 December 2013

DOI 10.1002/pros.22775

Published online 12 February 2014 in Wiley Online Library (wileyonlinelibrary.com).

## INTRODUCTION

Prostate cancer (CaP) causes substantial morbidity and mortality worldwide and remains the second most common cancer in older men and accounts for an estimated 33,720 deaths in the United States in 2011 [1]. Localized CaP patients have a long-term survival due to great advances in surgical resection and radiotherapy (RT). However, patients with advanced and metastatic disease are often associated with a poor prognosis; up to 30% of treated patients suffer a relapse within 18 months after surgical resection. While initially responsive to androgen deprivation therapy, almost all CaP patients will inevitably progress to recurrent castration-resistant prostate cancer (CRPC) and die from secondary diseases (metastases).

RT continues to be one of the most popular treatment options for CaP patients detected at early-stage or advanced-stage disease. Up to 20% of localized CaP cases are considered high-risk, defined as T3-4 or Gleason score 8–10 or baseline prostate specific antigen (PSA) >20 ng/ml. For these high-risk cases, surgery or RT alone leads to high rates of local and distant relapse [2], which results in cancer progression to metastatic disease. One main reason for these failures following RT is due to the radioresistance of a subpopulation of CaP clones within the tumor. Radioresistance is a major challenge in current CaP radiation therapy. Thus, it is urgent and important to identify novel therapeutic targets to improve CaP radiosensitivity and overcome radioresistance.

Chemotherapy remains the main treatment option in the setting of CRPC, providing very modest survival benefits. Two docetaxel (DTX)-based clinical trials have unraveled the potential benefits of chemotherapy to prolong the survival time and improve the quality of life in CaP patients for the first time, at the cost of significant toxicity [3,4]. Although newer chemotherapeutics such as satraplatin and cabazitaxel have demonstrated activity, survival benefits are still modest [5,6]. Its effectiveness is largely challenged by the drug-resistant nature of CaP. Hence, it is important to investigate the underlying mechanisms and signaling pathways involved in CaP metastasis and progression and identify novel and effective therapeutic targets to improve current therapeutic modalities.

CD44 is an 85–90 kDa transmembrane glycoprotein receptor composed of four functional domains, which serves as a cellular adhesion molecule for hyaluronic acid (HA), a major component of the extracellular matrix [7]. The proximal extracellular domain of CD44 is the site of alternative splicing for CD44 mRNA that produces different variant isoforms of CD44. While the standard isoform of CD44 (CD44std) is expressed

predominantly in normal epithelial cell subsets [8], CD44 variant isoforms (CD44v), which contain additional insertions, are highly expressed in many epithelial-type carcinomas [7]. Expression of CD44v has been closely linked to tumor progression, metastasis, and treatment resistance processes in various cancers [9]. In particular, the variant CD44 molecule containing exon 10, also known as CD44 variant 6 (CD44v6) is closely associated with aggressive behavior and correlates with poor prognosis in a variety of human malignancies including breast cancer [10], leukemia [11], gastric cancer, [12] and colorectal cancer [13], and it has been shown to regulate malignant transformation by inducing tumor cell proliferation, adhesion, and migration [10,14]. Overexpression of CD44v6 was reported as a poor prognostic factor in some human malignant tumors [15,16]. On the other hand, other studies found that loss of expression of CD44v6 was correlated with poor prognosis [17,18]. These conflicting results suggest an elusive role of CD44v6 in cancer progression and metastasis. The roles and functions of CD44v6 in CaP metastasis and progression are still uncertain. Therefore, investigation of CD44v6 in CaP metastasis and progression, and association with cancer cell stemness may provide promising insights for the development of novel therapeutic strategies for CaP.

In the current study, we demonstrate for the first time that in CaP CD44v6 has stem cell-like properties and is closely associated with CaP proliferation, invasion, metastasis, chemo-/radioresistance, inducing epithelial–mesenchymal transition (EMT) as well as the activation of PI3K/Akt/mTOR and Wnt signaling pathways. Our findings have significant clinical implications and demonstrate that CD44v6 may prove to be a useful therapeutic target to improve CaP chemo-/radiosensitivity for future CaP therapy.

## MATERIALS AND METHODS

### Sample Collection

Ethical approval was obtained from the South East Health Human Research Ethics Committee, South Section, Sydney, Australia. Primary CaP tissues (n = 10) from patients undergoing radical prostatectomy (RP), lymph node metastases (n = 10), and BPH tissues (n = 10), and normal prostate biopsies (n = 10) were obtained at Urology Sydney, St George Private Hospital, Sydney, Australia from 2000 to 2005.

### Antibodies and Reagents

Antibodies were purchased from different sources. The detailed information and conditions are listed in

**TABLE I. Antibodies Used for Immunofluorescence (IF) Staining and Western Blot (WB)**

Antibody	Source	Type	Dilution	Incubation time (min)	Temperature	Application
Mouse anti-human CD44v6	Abcam	MAb	1:1,000 (WB)1:100 (IHC, IF)	O/N	4°C	WB, IHC, IF
Mouse anti-human CD44std	eBioscience	MAb	1:500 (WB)1:50 (IF)	O/N	4°C	WB, IF
Rabbit anti-human E-cadherin	Epitomics, Inc.	MAb	1:2,000 (WB)	O/N	4°C	WB
Rabbit anti-human Vimentin	Epitomics, Inc.	MAb	1:2,000 (WB)	O/N	4°C	WB
Rabbit anti-human SNAIL	Abcam	PAb	1:1,000 (WB)	O/N	4°C	WB
Rabbit anti-human SLUG	Abcam	PAb	1:1,000 (WB)	O/N	4°C	WB
Rabbit anti-human Twist	Abcam	PAb	1:1,000 (WB)	O/N	4°C	WB
Rabbit anti-human Akt	Abcam	PAb	1:1,000 (WB)	O/N	4°C	WB
Rabbit anti-human p-Akt	Abcam	PAb	1:1,000 (WB)	O/N	4°C	WB
Rabbit anti-human mTOR	Cell Signaling	PAb	1:1,000 (WB)	O/N	4°C	WB
Rabbit anti-human p-mTOR	Cell Signaling	PAb	1:1,000 (WB)	O/N	4°C	WB
Rabbit anti-human S6k	Abcam	MAb	1:1,000 (WB)	O/N	4°C	WB
Rabbit anti-human p-S6k	Abcam	PAb	1:1,000 (WB)	O/N	4°C	WB
Rabbit anti-human 4EBP1	Cell Signaling	MAb	1:1,000 (WB)	O/N	4°C	WB
Rabbit anti-human p-4EBP1	Cell Signaling	MAb	1:1,000 (WB)	O/N	4°C	WB
Rabbit polyclonal IgG Isotype Control	Abcam	PAb	1:100 (IHC, IF)	O/N	4°C	IHC, IF
Mouse anti-human GAPDH	Merck Millipore	PAb	1:600 (WB)	O/N	4°C	WB
Goat anti-mouse Alexa Fluor <sup>®</sup> 488 Dye Conjugate	Invitrogen	IgG	1:1,000 (IF)	60	RT	IF
Goat anti-rabbit IgG-HRP	Santa Cruz Biotechnology	PAb	1:2,500 (WB)	60	RT	WB
Goat anti-mouse IgG-HRP	Santa Cruz Biotechnology	PAb	1:2,500 (WB)	60	RT	WB
Swine anti-goat, mouse, rabbit IgG/Biotinylated	Dako Cytomation	PAb	1:450 (IHC)	45	RT	IHC

HRP, horseradish peroxidase; IF, immunofluorescence; MAb, monoclonal antibody; O/N, overnight; PAb, polyclonal antibody; RT, room temperature; WB, Western blot; IHC, Immunohistochemistry.

Table I. DTX, Paclitaxel (PTX), Doxorubicin (DOX), and Mitoxantrone (MTX) were purchased from Sigma-Aldrich, Pty Ltd. (Castle Hills, NSW, Australia). The DTX, PTX, and MTX were first diluted in 100% ethanol while DOX was diluted in DMSO, and the four drugs were added to the growth medium when performing the following experiments as shown in Figure S1. The final concentrations of 100% ethanol or DMSO used in all experiments were 0.01%. siRNAs targeting CD44v6 and a scrambled (scr) sequence control for off-target effects were obtained from Sigma-Aldrich Pty Ltd. Insulin, B27, EGF, and bFGF were purchased from Invitrogen Australia Pty Ltd. (Melbourne, VIC, Australia).

### Cell Lines and Cell Culture

Androgen-non-responsive (PC-3, PC-3M, DU145, LNCaP-C4-2B), androgen-responsive (LNCaP, LNCaP-LN3, DuCaP) CaP cell lines, and normal prostate epithelial cell line (RWPE-1) from different sources

were studied (Table SI). All cell culture reagents were supplied by Invitrogen Australia Pty Ltd. unless otherwise stated. PC-3, PC-3M, DU145, C4-2B, and LNCaP cell lines were cultured in RPMI-1640 supplemented with 10% (vol/vol) heat-inactivated fetal bovine serum (FBS), 50 U/ml of penicillin and 50 µg/ml of streptomycin; LN3 cells in 1:1 RPMI-1640:F12-K; DuCaP cells in DMEM, and RWPE-1 cell line was cultured in Keratinocyte Serum Free Medium (K-SFM) supplemented with 0.05 mg/ml bovine pituitary extract and 5 ng/ml human recombinant epidermal growth factor (EGF). All cell lines were maintained in a humidified incubator at 37°C and 5% CO<sub>2</sub>.

PC-3, DU145, LNCaP, and RWPE-1 cell lines were obtained from American Type Culture Collection (ATCC, Rockville, MD). The PC-3M cell line was kindly provided by Dr C Power (Prince of Wales Hospital, UNSW, Australia); LN3 and C4-2B cell lines were kindly provided by Dr C Pettaway (M.D. Anderson Hospital, Austin, TX). DuCaP cell line was provided by Dr K Pienta (University of Michigan Comprehensive Cancer Center, Ann Arbor, MI).

### Immunofluorescence Confocal Microscope Analysis

Immunofluorescence staining was performed as previously described [19]. Briefly, cells grown on glass coverslips ( $10^5$  cells) were fixed with methanol, rinsed with Tris-buffered saline (TBS; pH 7.5) and incubated with a mouse anti-CD44v6 primary antibody (1:100 dilution) at 4°C overnight (o/n). After rinsing in TBS, cells were incubated in Alexa Fluor-488 goat anti-mouse IgG (1:1,000 dilution) for 45 min at room temperature and propidium iodide (PI) was used for nuclei staining. Negative controls were treated identically but incubated with a mouse isotype control. Immunofluorescence was then visualized using an FV300/FV500 Olympus laser scanning confocal microscope (Olympus, Tokyo, Japan).

### Immunohistochemistry

Standard immunoperoxidase procedure was used to visualize CD44v6 expression as previously published [20]. Briefly, paraffin-embedded slides were deparaffinized in xylene and rehydrated with various concentrations of ethanol. For the antigen retrieval, slides were immersed in 0.01 M citrate buffer (Thermo Fisher Pty Ltd., VIC, Australia), pH6, and heated in a boiling water bath for 15 min. Slides were then incubated with a mouse anti-CD44v6 monoclonal antibody (MAb; 1:100 dilution) or a mouse anti-CD44std MAb (1:50 dilution) for 1 hr at room temperature. After washing with TBS, the slides were incubated with a biotinylated secondary antibody (1:300 dilution) for 45 min at room temperature, rinsed in TBS and then incubated in streptavidin/horseradish peroxidase (HRP; 1:300 dilution) for 30 min at room temperature. After rinsing in TBS, immunoreactivity was developed with 3,3'-diaminobenzidine (DAB) substrate (Thermo Fisher Pty Ltd.) containing 0.03% hydrogen peroxide (VWR International, QLD, Australia) and counterstained with Harris Hematoxylin (Thermo Fisher Scientific) for 1 min. Negative controls were treated identically but with the primary antibody omitted.

### Western Blot

Protein expression levels were evaluated by Western blot as previously described [21]. Briefly, whole cell lysates were run on NuPAGE Novex 4-12% Bis-Tris gel and then transferred to polyvinylidene difluoride (PVDF) membrane. After blocking non-specific sites with 5% bovine serum albumin (BSA) in Tris-buffered saline with 0.1% Tween 20 (TBST), the membrane was incubated with different primary anti-

bodies (see Table I) at 4°C o/n, followed by incubation with HRP-conjugated secondary antibodies. Immunoreactive bands were detected using enhanced chemiluminescence (ECL) substrate (Pierce Chemical Co., Rockford, USA), and visualized using the ImageQuant LAS4000 system (GE Healthcare, USA). To confirm the equality of protein lysates loading, membranes were stripped using Restore Western Blot Stripping Buffer (Pierce Chemical Co.), and re-probed using a rabbit anti-human GAPDH PAb, then processed as above.

### Short Interfering RNA (siRNA) Transfection

CaP cells were knocked down (KD) by CD44v6-siRNAs or CD44v6-scr-siRNA using LipofectAMINE 2000 (Invitrogen) following the manufacturer's protocol. Incubation time with siRNA or scr complex was 72 hr with each cell line as a published method [22].

### RNA Extraction

Approximately  $4 \times 10^5$  cells from CD44v6-KD, CD44v6-scr, and untreated control CaP cell lines were trypsinized, rinsed with PBS and centrifuged. The total RNA was extracted and purified using the RNeasy Plus Mini Kit (Qiagen, VIC, Australia) according to the manufacturer's instructions. The concentrations of total RNA from each cell line were measured by a ND-2000 NanoDrop spectrophotometer (NanoDrop Technologies, Wilmington, DE).

### Quantitative Real-Time PCR

Two micrograms ( $\mu\text{g}$ ) of total RNA from each cell line were reverse transcribed to cDNA using the SuperScript III First-strand Synthesis System Kit (Invitrogen Pty Ltd.), according to the manufacturer's protocol. Quantitative real-time PCR (qRT-PCR) was used for the assessment of mRNA expression of the CD44v6 gene. It was carried out in a solution containing 12.5  $\mu\text{l}$  SYBR<sup>®</sup> Select Master Mix (Applied Biosystems, VIC, Australia), 2.8  $\mu\text{l}$  TaqMan<sup>®</sup> Gene Expression Assay (CD44v6, sense, 5'-TCCCAGTATGACACATATGTC; antisense, 5'-CCCACATGCCATCTGTTGCC), 7.3  $\mu\text{l}$  of nuclease-free water and 2.5  $\mu\text{l}$  of cDNA sample in a final volume of 20  $\mu\text{l}$ . GAPDH (Hs02758991\_g1) was used as an endogenous control. A Rotor-Gene instrument (Corbett Life Science, Sydney, Australia) was used for automated qRT-PCR setup of the reactions. After three independent experiments, the REST 2009 V2.0.13 (Qiagen) software was used for calculation and analysis of CD44v6 gene expression.

### Proliferation Assay

Proliferating capacity of CD44v6-KD, CD44v6-scr, and control CaP cells was determined using a CyQUANT<sup>®</sup> NF Cell Proliferation Assay Kit (Invitrogen) according to the manufacturer's instructions. Briefly, 1,000 cells in 100  $\mu$ l complete medium were seeded in 96-well plates and incubated at 37°C and humidified 5% CO<sub>2</sub>. The growth medium was then removed and cells were dyed with the dye binding solution in the kit. The fluorescence intensity of each sample was measured using a BIO-TEK fluorescence microplate reader (Bio-Rad, Hercules, CA) with excitation at ~485 nm and emission at ~530 nm in the following consecutive 7 days. The average fluorescence intensity of each cells for each day was plotted (mean  $\pm$  SD, n = 3).

### Colony Formation Assay

CD44v6-KD, CD44v6-scr, and control CaP cells were used for colony forming assay as previously described with minor modifications [23]. Briefly, 1,500 cells/dish were seeded in 10 cm dishes and incubated in a humidified incubator at 37°C with 5% CO<sub>2</sub>. The media were replaced regularly and all cultures were incubated for 10 days until the colonies were large enough to be clearly discerned. The colonies, defined as groups of >50 cells, were scored manually with the aid of an Olympus INT2 inverted microscope (Olympus, Tokyo, Japan). The average numbers of colonies were plotted (mean  $\pm$  SD, n = 3).

### Cell Adhesion Assay

Briefly,  $2 \times 10^5$  CD44v6-KD, CD44v6-scr, and wild type CaP cells were seeded in 96-well plates previously coated with high molecular weight HA (Sigma-Aldrich Pty Ltd., Australia) and blocked with 2% BSA in PBS, respectively, and followed by incubation for 1 hr. After washing with PBS three times, adherent cells were measured using CyQUANT<sup>®</sup> NF Cell Proliferation Assay Kit (Invitrogen) according to the manufacturer's instructions. Fluorescence intensity of each well was measured using a BIO-TEK fluorescence microplate reader (Bio-Rad) with excitation at ~485 nm and emission at ~530 nm. The average fluorescence intensity of each cell was recorded (mean  $\pm$  SD, n = 3).

### Matrigel Invasion Assay

Invasive ability of CD44v6-KD, CD44v6-scr, and control CaP cells was assessed using commercial matrigel and control transwell chambers (BD Biosci-

ence). Briefly,  $2 \times 10^4$  cells in 500  $\mu$ l serum-free RPMI-1640 medium were added to each transwell insert, respectively. Seven hundred fifty microliter of complete medium was added to the outer wells to provide chemoattractant and prevent dehydration. Cells were incubated at 37°C and humidified 5% CO<sub>2</sub> for 48 hr and then stained with a Diff-Quik staining kit (Allergiance Healthcare Corp., Illinois, USA). The number of stained cells that invaded through the matrigel or control inserts was counted in five high power fields by light microscope (Leica Microscope, Nussloch, Germany). The ability of invasion was calculated as follows: Invasion ratio = [Mean cells invading through matrigel insert / Mean cells migrating through control insert]  $\times$  100%. Cell invasion ratios were plotted (mean  $\pm$  SD, n = 3).

### Sphere Formation Assay

Cells were trypsinized, dissociated into single cells and then plated into an ultra low attachment round-bottom 96-well-plate (Sigma-Aldrich Pty Ltd.). Final cell dilution ranging from 1 to 100 cells in 100  $\mu$ l serum-free DMEM/F12K media supplemented with 4  $\mu$ g/ml insulin, B27, and 20 ng/ml EGF and bFGF were added into each well. Spheres that arose following a 7-day incubation were counted. The diameters of each sphere were observed and measured by an inverted phase microscope (CK-2, Olympus, Tokyo, Japan) fitted with an ocular eyepiece after 5 days. Sphere formation capacity was assessed as the number of spheres with the diameter of >100  $\mu$ m.

### MTT Assay for Chemodrug Response

MTT assay was performed as described previously [21]. Briefly, 2,000 cells were seeded in 96-well plates and treated with a range of concentrations of DTX, PTX, DOX, and MTX which are commonly used in CaP chemotherapy. After 72 hr incubation, the media were replaced with fresh medium containing 0.5 mg/ml MTT [(3-(4,5-dimethylthiazol-2-yl)-2,5-diphenyltetrazolium bromide)]. The absorbance (OD) was read at a wavelength of 562 nm on a BIO-TEK microplate reader (Bio-Rad). The growth inhibition curve was generated using the GraphPad Prism 4 (GraphPad, San Diego, CA). Absolute IC<sub>50</sub> values for the four drugs were calculated using the intersection of the 50% normalized drug response and the growth inhibition curves for each cell line, to find the X-axis of IC<sub>50</sub> for DTX, PTX, DOX, and MTX, respectively.

### Chemosensitivity Assay

Briefly, 1,500 cells/dish were seeded in 10 cm dishes for 48 hr at 37°C and 5% CO<sub>2</sub> and then treated with a

fixed dose (1/2 dose of the  $IC_{50}$ ) of DTX, PTX, DOX, and MTX, respectively from the MTT assay in CD44v6-KD, CD44v6-scr, and wild type control CaP cells, or the same volume of vehicle control (100% ethanol for DTX, PTX, and MTX groups, and DMSO for DOX groups). The low dose chosen was based on our previous similar study. After 3 days treatment, the drug-containing media was replaced with fresh media and all cultures were incubated for an additional 7 days until colonies were large enough to be clearly distinguished. The scoring and statistical process was carried out as previously described [24]. The treatment protocol details are shown in Figure S1.

### Radiosensitivity Assay

Briefly, 1,000 cells/flask were seeded in 25 cm<sup>2</sup> flasks at 37°C and humidified 5% CO<sub>2</sub>. CD44v6-KD, CD44v6-scr, and wild type control CaP cells were exposed to a single dose (4 Gy) irradiation using a linear accelerator (Elekta, Stockholm, Sweden) at a dose rate of 2.7 Gy/min with 6 MV photons (Cancer Care Centre, St George Hospital, Sydney, Australia). The colony formation assay was then carried out in radiation-treated and untreated cells using a published method [22]. The media were replaced regularly and all cultures were incubated for 10 days until the colonies were large enough to be clearly distinguished. The colonies, defined as groups of >50 cells, were scored manually with the aid of an Olympus INT2 inverted microscope (Olympus, Tokyo, Japan). The average numbers of colonies were plotted (mean ± SD, n = 3).

### Assessment of Immunostaining

Staining intensity (0–3) in CaP cell lines and in CaP tissues was assessed using a confocal microscope (Olympus) and a light microscopy (Leica, Germany), respectively. The criteria used for assessment of CaP tissues were as previously reported [25], where: 0 (negative, <25%); 1+ (weak 25–50%); 2+ (moderate 50–70%); 3+ (strong >75%) of the tumor cells stained. Evaluation of cell and tissue staining was performed independently by two experienced observers (J.N. and Y.L.). All specimens were scored blind and an average of grades was recorded finally.

### Statistical Analysis

All numerical data were expressed as the average of the values (mean), and the standard deviation (SD) was calculated. Data from different groups were compared using the two-tail *t*-test. All *P* values were two-sided. *P* < 0.05 was considered significant. All

numerical statistical analyses were performed using the GraphPad Prism 4.00 package (GraphPad).

## RESULTS

### Expression of CD44v6 and CD44std in Metastatic CaP Cell Lines

Immunofluorescence labeling of CaP cells and RWPE-1 cells with anti-CD44v6 MAb showed positive staining in PC-3, PC-3M, DU145, C4-2B, LNCaP, LN3, and DuCaP cells, with variation between cell lines (Fig. 1A). Strong (Grade 3) expression of CD44v6 was seen in PC-3M, DU145, LNCaP, C4-2B, and LN3 cell lines. Medium (Grade 2) expression of CD44v6 was seen in PC-3 cell line. Low (Grade 1) expression of CD44v6 was found in DuCaP cell lines. Negative expression of CD44v6 was detected in RWPE-1 cell line. Expression of both membrane and cytoplasm was found in all positive CaP cell lines. The immunostaining grades are summarized in Table SI. The immunofluorescence results for the expression of CD44v6 in CaP cell lines and RWPE-1 cell line were further confirmed by Western blot (Fig. 1B). CD44std was found negatively to weakly expressed in CaP cell lines, whereas moderately expressed in RWPE-1 normal prostate cell line (Fig. 1B).

### Expression of CD44v6 and CD44std in Primary CaP Tissues, Lymph Node Metastases, BPH, and Normal Prostate Tissues

Immunoreactivity identified in primary CaP tissues, lymph node metastases, BPH, and normal prostates using paraffin sections stained with CD44v6 antibody is summarized in Table II. Typical staining results are shown in Figure 1C. In primary CaP tissues, strong CD44v6 expression was found in 9 out of 10 (90%) and moderate CD44v6 expression in 1 out of 10 (10%). In lymph node metastases, strong CD44v6 expression was found in 10 out of 10 (100%). The staining of CD44v6 in primary CaP tissues and lymph node metastases is both membrane and cytoplasm with more heterogeneous patterns. The CD44v6 expression is also strongly positive in stromal cells in both primary CaP tissues and lymph node metastases (see arrows; Fig. 1C). In the BPH samples, 3 out of 10 (30%) BPH tissues was found negative, 7 out of 10 (70%) were weakly positive to CD44v6. The positive staining in BPH was found mostly in epithelial cells but not in stromal cells and was heterogeneous. The positive staining was prominently associated with the cell membrane and the cytoplasm. Normal prostate tissues were weakly positive (1 out of 10) to negative (9 out of 10) for CD44v6 expression. In terms of CD44std

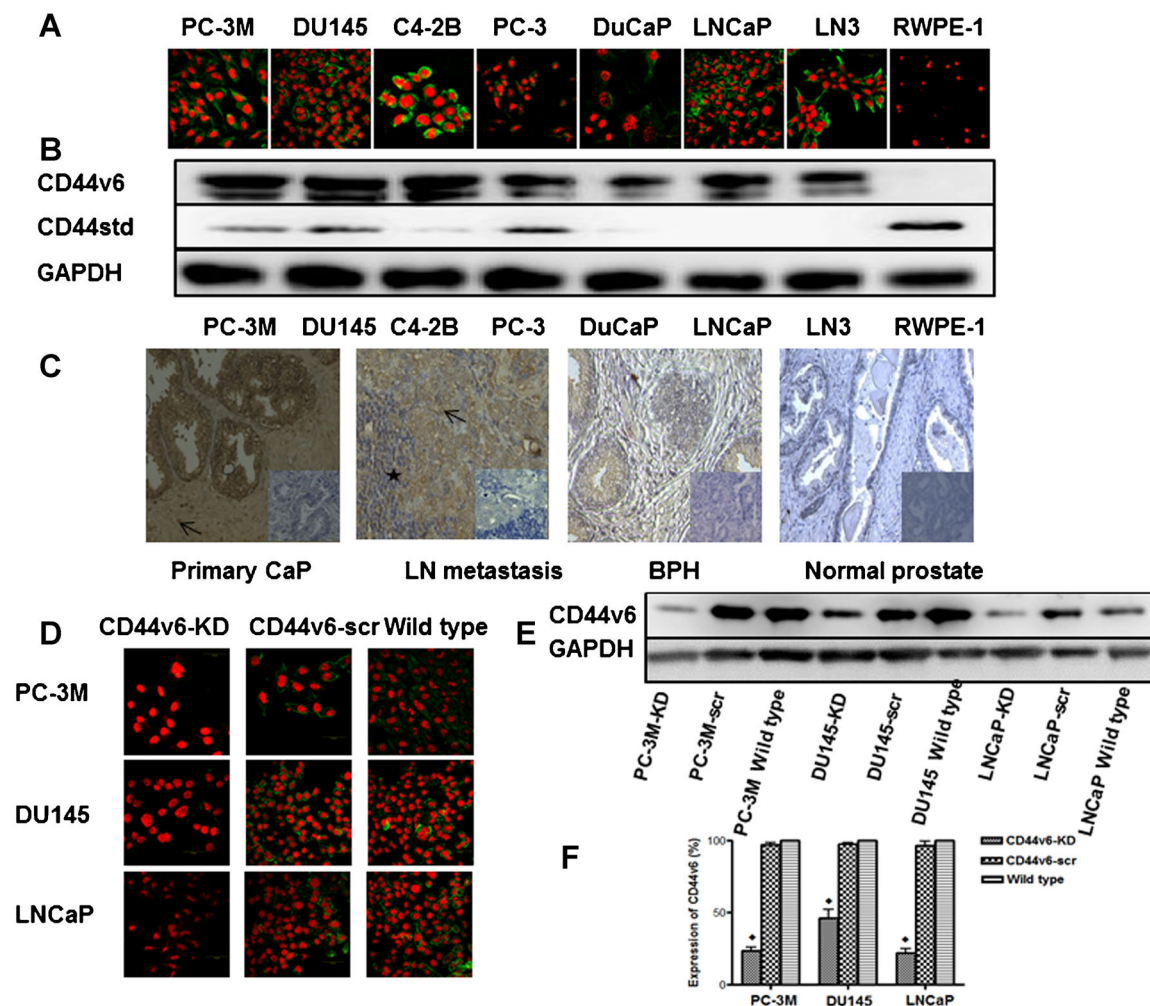


**Fig. 1.** Expression of CD44v6 and CD44std in metastatic CaP cell lines, normal prostate cell line, primary CaP tissues, and lymph node metastases and down-regulation of CD44v6 by CD44v6-siRNA in metastatic CaP cells. **A:** Representative immunofluorescence images of CD44v6 (green) in CaP cell lines and normal prostate cell line (RWPE-1). Nuclei are stained with PI (red). Magnification: all images  $\times 400$ . **B:** Western blot is shown to confirm the immunofluorescence staining in all CaP cell lines for CD44v6 expression and compare CD44v6 expression to CD44std expression. GAPDH was chosen as a loading control. **C:** Representative images of CD44v6 (brown) in primary CaP tissues and matched lymph node metastases (the lymph node in the image is from the same patient), BPH tissues and normal prostate tissues by immunohistochemistry. Nuclei are stained with Harris Hematoxylin (blue). Arrows indicated positive staining for surrounding stromal cells. Asterisk denotes lymphocytes. Magnification: all images (including insets)  $\times 400$ . **D:** Representative immunofluorescence images of CD44v6 (green) in the selected PC-3M, DU145, and LNCaP cell lines for KD study. Nuclei are stained with PI (red). Magnification: all images  $\times 400$ . CD44v6 expression in KD groups is obviously reduced compared to scr and wild type CaP control groups. **E,F:** Knock-down effects are further confirmed by Western blot and qRT-PCR ( $\blacklozenge$  indicates  $P < 0.01$ ). All results were from three independent experiments (mean  $\pm$  SD,  $n = 3$ ). BPH, benign prostatic hyperplasia; CaP, prostate cancer; KD, knock-down; LN, lymph node; PI, propidium iodide; scr, scrambled siRNA control.

expression, negative CD44std expression was found in all primary CaP tissues ( $n = 10$ ) and lymph node metastases ( $n = 10$ ), while in all normal prostate tissues ( $n = 10$ ), the CD44std expression is strongly positive (data not shown).

#### Expression of CD44v6 in CaP-KD and CaP-Control Cells

To further investigate the roles of CD44v6 in CaP metastasis and progression, we selected three CaP cell

lines (PC-3M, DU145, and LNCaP) with high level expression of CD44v6 for gene knock-down study. After knocking down CD44v6, the reduction of CD44v6 expression was significant in all three CaP cell lines compared to the negative control with a scrambled sequence and a wildtype control (Fig. 1D). No detectable staining was seen in the cells incubated with isotype control (data not shown). The immunofluorescence staining intensity in different CaP cell lines is summarized in Table SII. The immunofluores-

**TABLE II. Immunostaining Results for Normal Prostates, BPH Tissues, Different Human Prostate Tissues, and LN Metastases for CD44v6 Expression**

Tissue type	N	Tissue staining intensity			
		+++	++	+	-
Normal	10	0	0	1	9
BPH	10	0	0	7	3
CaP (G > 7)	10	9	1	0	0
LN. metastasis	10	10	0	0	0

BPH, benign prostatic hyperplasia; CaP, primary prostate cancer; G, Gleason score; LN, lymph node; N, number; -, negative; +, weak; ++, moderate; +++, strong.

cence staining results in different CaP cell lines after KD were further confirmed by Western blot (Fig. 1E) and qRT-PCR (Fig. 1F). The relative mRNA level of CD44v6 decreased to 6.3%, 18.6%, and 10.2% in PC-3M, DU145, and LNCaP CD44v6-KD cells, respectively.

#### Knock Down of CD44v6 Reduces Proliferative, Clonogenic, and Adherent Ability in CaP Cells

To investigate the proliferative ability after knocking down CD44v6, the cell numbers were observed for 7 days. Compared to scr and wild type control cell lines, the cell numbers in CD44v6-KD cell lines were significantly decreased ( $P < 0.05$ ; Fig. 2A) whereas no significant difference was found between scr and wild type cells ( $P > 0.05$ ).

To investigate whether KD of CD44v6 affects the growth potential of CaP cells, we assessed the colony formation in CD44v6-KD, CD44v6-scr, and wild type-control CaP cells. Our results indicated that the number of colonies in CD44v6-KD cells was significantly decreased by 46.0%, 40.5%, and 36.3% compared with that in PC-3M-scr, DU145-scr, and LNCaP-scr cells, respectively ( $P < 0.05$ ) while there was no significant difference between the colonies generated from CD44v6-scr control and wild type cells ( $P > 0.05$ ; Fig. 2B). Representative images for colony formation in different groups are shown in Figure S2A.

Attachment of CaP cells to the extracellular matrix is necessary for cell motility and invasion. Therefore, it is important to test the role of CD44v6 in adhesion to HA-coated and -uncoated well plates. As shown in Figure 2C, CD44v6-KD cell lines showed a significant decrease of 36.1%, 27.0%, and 39.5% in adherent ability compared to PC-3M-scr, DU145-scr, and LNCaP-scr cell lines, respectively ( $P < 0.05$ ) while no significant

difference was observed between CD44v6-scr cells and wild type cells ( $P > 0.05$ ).

#### Knock Down of CD44v6 Reduces CaP Cell Invasion and Tumor Sphere Forming Ability

To further test the causal relationship of CD44v6 and invasion, we proceeded to downregulate CD44v6. After knocking down CD44v6, cell invasion was significantly reduced by 52.2%, 50.2%, and 59.5% in KD cells compared to PC-3M-scr, DU145-scr, and LNCaP-scr cells, respectively ( $P < 0.05$ ), while there was no significant difference between scr and wild type control cells ( $P > 0.05$ ; Fig. 2D). The average percentage of invasion for each subline is summarized in Table SII. Representative images for each subline are shown in Figure S2B.

To assess the relative presence of sphere-forming cells in a cell population, a range of 1–100 CaP cells from each subline were calculated using a linear regression of wells without spheres by a published method [26]. The mean X-intercept value of the graph indicates the number of cells needed to form one sphere per well, which was much higher in the CD44v6-KD cells, when compared to the CD44v6-scr and wild type control groups ( $P < 0.01$ ), while there was no significant difference between CD44v6-scr and wild type control groups ( $P > 0.05$ ), suggesting that knocking down of CD44v6 reduces the relative number of cells capable of forming spheres in the population of three CaP cell lines (Fig. 3A). Morphologically, the spheres formed in KD groups tended to be looser and smaller than those in the control and wild type groups. Representative images for KD, scr, and wild type control cells are shown in Figure 3B.

#### Cytotoxicity of Chemodrugs in CaP Cells In Vitro

The effect of DTX, PTX, DOX, and MTX treatment on single cell cytotoxicity was assessed by MTT assay. Our results indicated a dose-independent cell proliferation inhibition of DTX, PTX, DOX, and MTX on PC-3M-scr, DU145-scr, and LNCaP-scr CaP cells. Each cell line displayed a variable response to different drugs and no cytotoxic effect was found for vehicle control in all cell lines tested (data not shown). The PC-3M-scr cell line is the most sensitive to PTX ( $IC_{50}$ : 4.8 nM); the DU145-scr cell line is the most sensitive to DTX ( $IC_{50}$ : 8.3 nM); the LNCaP-scr cell line is the most sensitive to PTX ( $IC_{50}$ : 1.5 nM). The  $IC_{50}$  values of each drug on each cell lines are summarized in Table SIII. The  $1/2$  dose of  $IC_{50}$  values from MTT assay were chosen for the following chemosensitivity study based on our previous similar study.

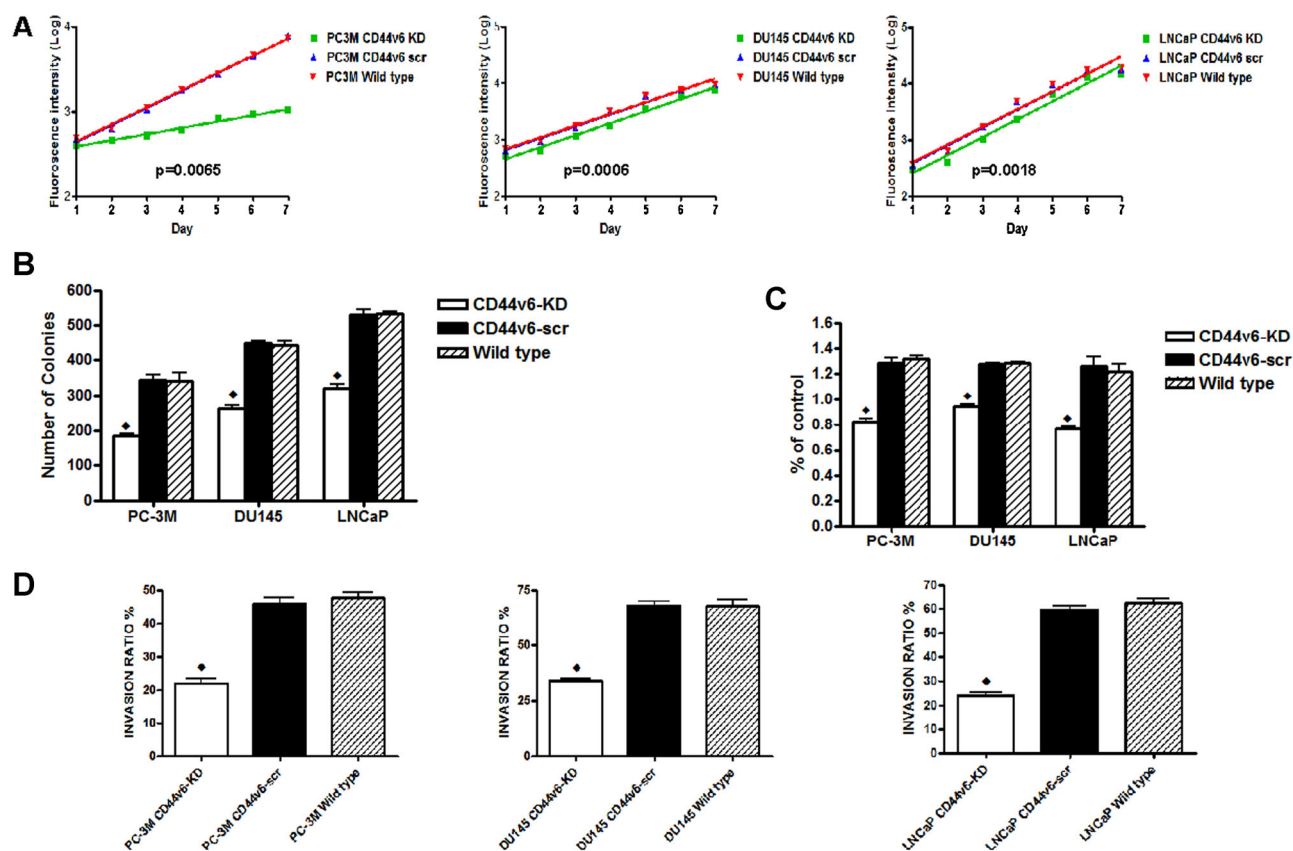


**Fig. 2.** Proliferation, colony formation, adhesion, invasion after knocking down CD44v6 in CaP cells. **A:** Proliferation rate in PC-3M, DU145, and LNCaP cells was significantly reduced in KD cells compared to scr and wild type control cells ( $P < 0.05$ ) while there was no significant difference between scr cells and wild type cells in three cell lines ( $P > 0.05$ ), respectively. **B:** Nine CaP cell lines (KD, scr, and wild type groups) were seeded in 100 mm dishes and cultured in growth medium for 10 days. Results are presented as the number of colonies formed. Significant decreases in colony formation were observed in KD group of PC-3M, DU145, and LNCaP cells, respectively, compared to the scr and wild type control groups (◆ indicates that  $P < 0.05$ ). **C:** Interaction of CD44v6 with HA mediates cell adhesion. KD groups in three cell lines showed a significant decrease in cell adhesion to HA, compared with scr and wild type groups, respectively (◆ indicates that  $P < 0.05$ ). **D:** After knocking down, the invasive potential was significantly reduced by 52.2%, 50.2%, and 59.5% in PC-3M-KD, DU145-KD, and LNCaP-KD cell lines compared to control cells, respectively (◆ indicates that  $P < 0.05$ ). All results were obtained from three independent experiments (mean  $\pm$  SD,  $n = 3$ ). HA, hyaluronic acid; KD, knock-down; scr, scrambled siRNA control.

### Knock Down of CD44v6 Increases CaP Cells Chemosensitivity and Radiosensitivity In Vitro

After treatment with  $1/2$  dose of  $IC_{50}$  values of each drug, three CD44v6-KD CaP cells demonstrated obviously reduced colony formation compared to CD44v6-scr cells, normalized by untreated control cells ( $P < 0.05$ ) (Fig. 4A). The most sensitive chemodrug in PC-3M-KD and LNCaP-KD cells is DTX, and the colony formation is 1.8% and 0.6% of untreated control group, respectively. The most sensitive chemodrug in DU145-KD cell is MTX, and the colony formation is 1.3% of untreated control group. The average percentage of colony formation in different CaP sublines after chemodrug treatment is summarized in Table SIV. These results suggest that knocking down CD44v6 significantly increases the chemosensitivity to DTX,

PTX, DOX, and MTX in PC-3M, DU145 and LNCaP CaP cells with some variations, and that the DTX is the most sensitive chemodrug among them. Typical images of colony formation to different chemodrugs in three CaP cell lines are shown in Figure S3.

After treatment by a single dose of 4 Gy irradiation, three CD44v6-KD CaP cells showed significant reduction in colony formation, compared to CD44v6-scr and wild type control cells as well as untreated control cells ( $P < 0.05$ ; Fig. 4B). Although 4 Gy radiation treatment caused a reduction in colony formation in CD44v6-scr and wild type controls, no significant difference was found between these two controls (CD44v6-scr and wild type treated with radiation) with the untreated CaP control ( $P > 0.05$ ; Fig. 4B). The most radiosensitive CaP-KD cell line is LNCaP cells and the colony formation accounts for 22.7% of untreated cells after

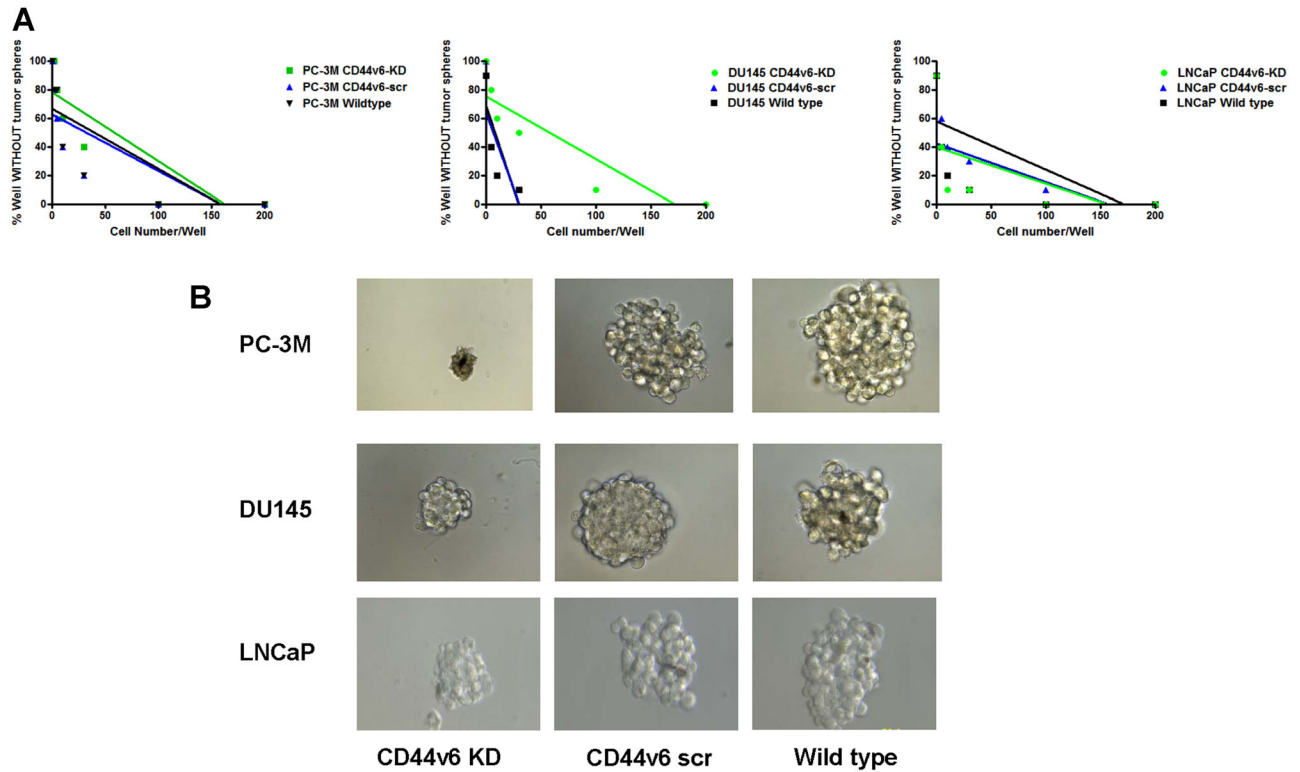


**Fig. 3.** Sphere formation after CD44v6 knock down in CaP cells. **A:** The mean X-intercept values calculated from limiting dilution analysis for each cell subtype reveal that the number of cells required to form at least one tumor sphere/well was much higher in KD groups, compared to the scr and wild type groups ( $P < 0.05$ ). **B:** Representative images for CaP tumorsphere formation in KD and control cells are shown by light microscope. Magnification  $\times 400$  in all images. Morphologically, the spheres formed in KD groups tended to be looser and smaller than those in the control and wild type groups. All results were obtained from three independent experiments (mean  $\pm$  SD,  $n = 3$ ). CSC, cancer stem cells; KD, knock-down.

radiation treatment. The average percentage of colony formation in different CaP sublines after RT is summarized in Table SV. These findings indicate that the KD of CD44v6 increases the radiosensitivity of PC-3M, DU145, and LNCaP CaP cells. Typical images of colony formation to RT in three CaP cell lines are shown in Figure S4.

#### EMT, PI3K/Akt/mTOR, and Wnt/ $\beta$ -catenin Signaling Pathways Related to the Expression of CD44v6 in CaP Cells

To further investigate whether EMT and some signaling pathways are involved in the effects of KD CaP cells, we examined several EMT and signaling pathway proteins. Our results demonstrated that after knocking down CD44v6, the level of E-cadherin (EMT marker) was increased, while the expression of EMT proteins (Vimentin, Twist, Snail, and Slug), PI3K/Akt/mTOR signaling proteins (p-mTOR, p-Akt, p-4EBP1, t-S6K, and p-S6K) and Wnt/ $\beta$ -catenin signaling proteins ( $\beta$ -catenin and p- $\beta$ -catenin) were down-regulated compared to CD44v6-scr cells, whereas no obvious

changes were seen in t-mTOR, t-Akt, and t-4EBP1 expression in all CaP cell lines (Fig. 5). These data indicate that KD of CD44v6 is associated with the reduced EMT and inactivation of PI3K/Akt/mTOR and Wnt/ $\beta$ -catenin signaling pathways in CaP cells, suggesting that EMT and the two signaling pathways may be involved in the regulation of CaP metastasis and chemo-/radioresistance together with CD44v6.

#### DISCUSSION

In this study, we examined the expression of CD44v6 and CD44std in metastatic CaP cell lines, primary CaP, lymph node metastases, BPH, and normal prostate tissues to investigate the roles of CD44v6 in CaP metastasis, progression, chemo-/radioresistance, and the association with PI3K/Akt/mTOR and Wnt/ $\beta$ -catenin signaling pathways. High levels of CD44v6 were found in both androgen-nonresponsive (PC-3, PC-3M, DU145, and C4-2B) and androgen-responsive (LNCaP and LN3) metastatic CaP cell lines and in all specimens of primary CaP and lymph node metastases, but not in normal prostate

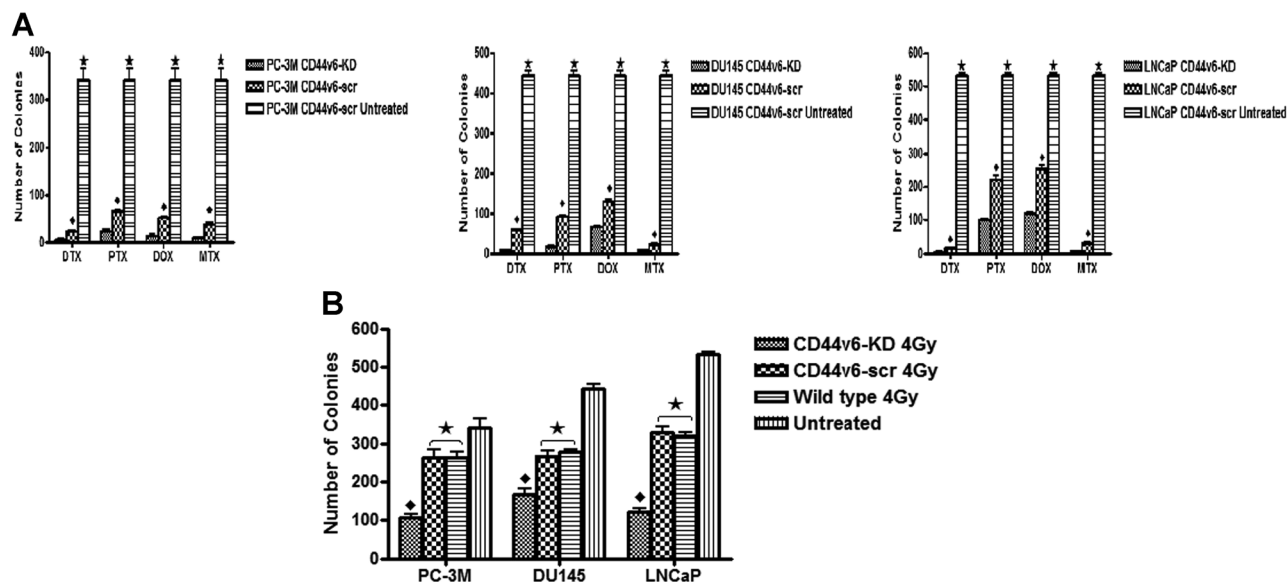


**Fig. 4.** Chemosensitivity and radiosensitivity after knocking down CD44v6 in CaP cells. **A:** Typical results are shown for colony formation in CaP cell lines treated with DTX, PTX, DOX, and MTX, “♦” indicates that the significant decreases in the average number of colonies were seen in CD44v6-KD cells compared to the CD44v6-scr and untreated cells in response to all three drugs tested ( $P < 0.05$ ). **B:** Results of radiosensitivity in colonies of CaP cell lines are shown. “♦” indicates a significant difference in the average number of colonies between CD44v6-KD cells and CD44v6-scr, wild type as well as untreated cells after irradiation ( $P < 0.05$ ). All results were obtained from three independent experiments (mean  $\pm$  SD,  $n = 3$ ). DOX, doxorubicin; DTX, docetaxel; KD, knock-down; MTX, mitoxantrone; PTX, paclitaxel; scr, scrambled siRNA control.

cells, BPH or normal prostate tissues. However, expression of CD44std was found negative or weak in metastatic CaP cell lines, negative in primary CaP tissues and lymph node metastases, but moderately positive in RWPE-1 normal prostate cell line and even strongly positive in all normal prostate tissues. Our observations indicate that CD44v6 may be involved in CaP progression in both early and late-stage events, which is further supported by a report that CD44v6 expression was seen in prostatic intraepithelial neoplasias (PIN) as well as in CaP lymph node metastasis [27]. On the contrary, in CD44std studies, it was reported that decreased CD44std is correlated with CaP metastasis in a Dunning rat model [28]. Furthermore, loss of CD44std was found to be correlated with poor prognosis in CaP patients [29,30]. These results suggest that CD44std may negatively regulate CaP progression, further supporting our observations. The weak expression of CD44std in PC-3M, DU145, and PC-3 cell lines may be attributed to the heterogeneity of CaP and gene alterations over cell passages or changes of microenvironment. In this study, we also found that high levels of CD44v6 expression were observed in both cancer cells and stromal cells in primary CaP tissues and lymph node metastases, suggesting that CD44v6 may be involved in the communication between CaP cells and tumor microenvironment to promote cancer cell invasion, migration,

metastasis, and therapeutic resistance. The exact mechanisms of the communication between cancer and stromal cells via CD44v6 in CaP are still unclear and will be investigated in our ongoing studies.

The results in CaP CD44v6 clinical studies were very variable from different research groups. Ekici et al. [31] found that CD44v6 expression was elevated in CaP patients who later had biochemical recurrence whereas Aaltomaa et al. [30] reported that CD44v6 is an independent predictor of survival of CaP patients. On the contrary, Noordzij et al. [29] reported that expression of CD44v6 is inversely correlated with prognosis of CaP patients treated by RP, and Takahashi et al. [32] found that CD44v6 has no correlation with CaP prognosis. In the current study, our findings support the idea that high levels of CD44v6 expression are associated with CaP progression and metastasis, which is conflicting with several previous studies [27,32] where decreased level of CD44v6 was observed in primary CaP tissues, and even weaker presentation in lymph node metastasis. The reasons for the conflicting results may be explained by the discrepancies in methodology such as experiment design, specimen selection, specificity of the antibodies, processing of the samples, patient population, different stages of samples chosen and the complexity of CaP itself. Due to the elusive roles of CD44v6 in different types of cancers including CaP, there is very limited data

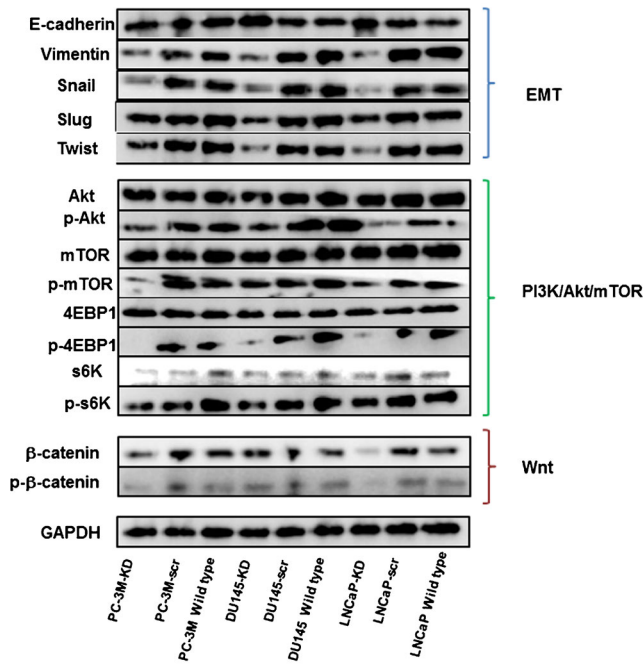


**Fig. 5.** The changes of EMT markers and PI3K/Akt/mTOR and Wnt signaling pathways proteins after knocking down CD44v6 in CaP cells. Representative results are shown for five markers (E-cadherin, Vimentin, Snail, Slug, and Twist) involved in EMT, eight signal transduction molecules (Akt, p-Akt, mTOR, p-mTOR, 4EBP1, p-4EBP1, S6K, and p-S6K) involved in PI3K/Akt/mTOR signaling pathway and two signal transduction molecules ( $\beta$ -catenin, p- $\beta$ -catenin) involved in Wnt/ $\beta$ -catenin pathway associated with CD44v6 expression in CaP. The level of E-cadherin was increased in all KD cell lines, while the levels of Vimentin, Snail, Slug, Twist, p-mTOR, p-Akt, p-4EBP1, p-S6K, and S6K were significantly reduced in all KD cell lines, compared to scr and wild-type controls. GAPDH was used as a loading control. KD, knock-down; p-4EBP1, phosphorylated-4EBP1; p- $\beta$ -catenin, phosphorylated- $\beta$ -catenin; p-Akt, phosphorylated-Akt; p-mTOR, phosphorylated-mTOR; p-S6K, phosphorylated-S6K; scr, scrambled siRNA control.

reported to demonstrate its roles in CaP progression and metastasis least of all the underlying signaling pathways involved. Therefore, understanding the roles of CD44v6 in CaP metastasis and related signaling pathways is critical and significant in developing novel targeted therapeutic approaches for the treatment of metastatic CaP.

In this study, after knocking down CD44v6 using siRNA, we found a decreased proliferation rate in three CD44v6<sup>+</sup> CaP cell lines, indicating that overexpression of CD44v6 is related to CaP growth and progression. Colony formation assay provides a more appropriate measure of long-term effects of therapeutic agents, assessing the ability of cells to retain their proliferative capacity after treatment, a characteristic that clinically facilitates tumor recurrences [24]. Our results show that silencing of CD44v6 suppressed the

survival potential of CaP cells, further validating the important role of CD44v6 in CaP growth, proliferation, and recurrence.

Tumor metastasis consists of three steps: adhesion, degradation, and metastasis [33]. Adhesion is the first and most important step to trigger tumor metastasis. Extracellular environment molecules such as HA (the ligand of CD44std and CD44v) which interacts with the distal portion of CD44 extracellular domain have been shown to play key roles in cancer metastasis [34]. Our results indicate that after knocking down CD44v6, CaP cells showed a significantly decreased adhesive ability to HA, suggesting that CD44v6 may play an important role in mediating tumor cell adhesion during the metastasis process. Matrigel invasion assay mimics the extracellular matrix environment by providing growth factors and creating a matrix scaffold for tumor cells to invade through. In this study, we found reduced invasion ability in all three CD44v6-KD cell lines, implying that CD44v6 is correlated with CaP cell invasion. One possibility for this reduced CaP invasion is that CD44v6 may promote invasion by up-regulating the activity of certain proteases, such as MMP-9 which is capable of digesting and degrading extracellular matrix components [35]. Another possible mechanism for the reduced invasive ability could be the down-regulation of EMT as this transition is essential in CaP metastasis [36].

EMT is characterized by the loss of epithelial characteristics and the gain of mesenchymal attributes and is a key event in tumor initiation via certain signaling pathways [37]. During EMT, epithelial cells downregulate cell-cell adhesion, lose their polarity and acquire a mesenchymal phenotype with increased interaction with the extracellular matrix as well as enhanced migratory capacity [38]. It was recently reported that the induction of EMT was accompanied by a shift in CD44 isoforms from CD44v to CD44s in breast cancer cells [39]. In this study, we have shown that silencing CD44v6 concomitantly downregulated EMT by loss of E-cadherin and upregulation of several key transcription factors. These findings are consistent with the reduced proliferation, adhesion, and invasion of CaP cells and implicates that CD44v6 may regulate these properties via EMT.

Over the past decade, CD44 was well documented as a common cancer stem cell (CSC) marker in many cancers including CaP [40–42]. CSCs, also known as tumor-initiating cells, are malignant cell subsets capable of tumor initiation and self-renewal and give rise to the bulk population of non-tumorigenic cancer cell progeny through differentiation [7]. They embody the refractory nature observed among many cancers: very competent initial tumor establishment, extremely aggressive metastatic nature, resistance to chemo-/

radiotherapy, correlation with advanced disease, and resistance to current therapies. Despite the ongoing debate on the abundance and origin of CSCs, it is generally accepted that they represent the root of cancer that must be eradicated in order to cure cancer. Although the origins of CSCs remain unclear in most types of cancers including CaP, cancer treatments that target CSCs through specific markers or signaling pathways critically involved in CSC function could potentially increase the efficacy of current forms of therapy.

Whether CD44std or CD44v is a CSC marker is still under debate. CD44std and CD44v play different roles in different cancers, which are also regulated by the tumor microenvironment. Recent studies demonstrated that CD44v6 is a CSC marker in bladder cancer [43], breast cancer [44], and brain cancer [45]. To our knowledge, very little attention has been paid to the stemness of CD44v6 in CaP. The sphere formation assay has been proposed as a valuable method for isolating cancer cells with conserved stemness determinants that are able to propagate in defined media [46,47]. Sphere formation best mimics the enrichment and proliferation of CSCs. It has been generally agreed that, like stem cells, the tumorsphere-forming cells from primary tumors such as breast cancer and ovarian cancer, are capable of proliferation, self-renewal, and higher tumorigenicity [48,49]. The anchorage-independent sphere culture of stem cells was instrumental in the study of adult CSCs including CaP [50]. In this study, we found that all three CD44v6<sup>+</sup> CaP cell lines can form spheres in an appropriate cell number, and that knocking down of CD44v6 significantly reduces tumor sphere formation ability. Given that the expression of CD44v6 was only found in CaP tissues and lymph node metastases but not in normal prostate tissues, our results support the idea that CD44v6 displays CSC-like properties and is closely associated with CaP stemness, providing a novel insight to the development of new therapeutic strategies for CaP.

As CSC plays an important role in chemotherapies and radiotherapy, and is responsible for tumor recurrence, based on our observation above, it is of great interest to investigate whether CD44v6 is involved in CaP chemo-/radioresistance. To date, very limited data has demonstrated the link between chemo-/radioresistance and CD44v6 expression in cancers. Our previous *in vitro* studies showed that overexpression of CD44v3-10 is associated with chemoresistance (DTX) [21] and overexpression of CD44 (CD44std and CD44v) is correlated with radioresistance [22] using CaP cell lines. However, we did not examine whether CD44std or CD44v is responsive for radioresistance. In the current study, we found that reducing CD44v6

expression can greatly improve chemosensitivity with the treatment of DTX, PTX, DOX, and MTX as well as radiosensitivity in all three CaP cell lines, suggesting that over-expression of CD44v6 is highly correlated with CaP chemo-/radiosensitivity, and targeting CD44v6 may increase the efficacy of chemodrugs, sensitize the tumor to RT as well as reduce the collateral toxicity.

CaP cells utilize multiple signaling pathways to propagate and invade during tumor progression and metastasis [51]. Among them, PI3K/Akt/mTOR pathway is a key pathway that has been linked to tumorigenesis, CSC, and resistance to therapy in CaP and other solid tumors [52,53], playing a crucial role in regulating basic cellular functions including growth, proliferation, and survival by inhibition of apoptosis [54]. Several lines of evidence indicate that this pathway is closely related with CSC biology [55]. Preclinical studies suggest that the PI3K/Akt/mTOR pathway is important in maintaining a CSC population [56] and in EMT in CaP cells [37,57]. Jijiwa et al. [45] found that CD44v6 regulates growth of brain CSC through the Akt pathway. Pfeil et al. [58] reported that following treatment with a PI3K inhibitor LY294002, chemosensitivity is improved in chemoresistant LNCaP-abl CaP cell line. Zhan et al. [53] suggest that treatment with Akt inhibitors prior to ionizing radiation treatment has potential benefit to patients with breast cancer. Wnt/ $\beta$ -catenin signaling pathway also participates in self-renewal, pluripotency, proliferation, and cell-fate determination [59,60]. As Wnt/ $\beta$ -catenin pathway is associated with the chromosome orientation during mitosis, its perturbations may lead to a mitotic disjunction typical of many cancer cells [61]. Yuan et al. [62] found that Wnt/ $\beta$ -catenin regulates livin, a member of inhibitors of apoptosis family, and prevents cell apoptosis and thus takes part in the development of tumor cell chemoresistance. RT leads to breaks in the DNA strands, but since apoptosis is blocked, the cell switches on reparation mechanisms and survives. In this study, we have shown that silencing CD44v6 concomitantly down-regulated PI3K/Akt/mTOR and Wnt/ $\beta$ -catenin signaling proteins, suggesting that the activation of both pathways is associated with CD44v6 expression. These findings are also consistent with reduced proliferation, cell adhesion, cell invasion, sphere formation, and increased chemo-/radiosensitivity after silencing CD44v6, further highlighting the potential of both pathways as targets for future treatment of CaP.

As discussed above, CD44v6 plays an important role in CaP metastasis and progression. The expression of CD44v6 is only found in primary human CaP tissues and lymph node metastases rather than normal prostate tissues, which makes itself an ideal candidate

for targeted therapy in the treatment of metastatic refractory CRPC. Most CD44v6-related target therapies are using an anti-CD44v6 antibody alone or an anti-CD44v6 antibody as a carrier to conjugate a toxic agent such as a chemodrug or radioisotope to specifically target cancer cells in various human malignancies. It was for the first time reported that MAb1.1ASML that targets specifically CD44v6 was effective in suppressing the formation of lung metastasis from a metastatic pancreatic cancer cell line (BSp73ASML) in an animal model study [63]. The first clinical trial using anti-CD44v6 antibody BJWA1 was published in 2000, with no drug-related adverse event and sensitive tumor uptake [64]. Our group has recently reviewed the different approaches referring CD44v6 antibody conjugates in clinical trials [9]. In addition to targeting CD44v6 proteins, directed therapy against CD44v6 gene is another option. Misra et al. delivered CD44v6 short hairpin RNA (shRNA)/nanoparticle within the colon tumor cells to perturb HA/CD44v6 interaction, resulting in reduction of adenoma growth in mice, with no evidence of toxicity to date [65]. Qian et al. [66] achieved suppression of pancreatic tumor growth by targeted arsenic delivery with anti-CD44v6 single chain antibody conjugated nanoparticles. These results imply that CD44v6-specific nanoparticles provide a highly efficient and safe platform for cancer therapy and could be of great potential benefit for future CaP combination therapies, especially for CRPC.

In summary, we have demonstrated that overexpression of CD44v6 was found in metastatic CaP cell lines, primary CaP tissues and lymph node metastasis; that CD44v6<sup>+</sup> CaP cells have CSC-like properties and CD44v6 is closely involved in CaP cell proliferation, adhesion, invasion and chemo-/radio-sensitivity and associated with the activation of EMT, PI3K/Akt/mTOR and Wnt pathways in vitro. Our findings shed a new light on a potential role of CD44v6 in CaP progression and metastasis, and lead to an expansion of repertoire of targeted therapy for metastatic and refractory CRPC.

#### ACKNOWLEDGMENTS

The authors thank Professor Pamela Russell and Dr Carl Power (Oncology Research Centre, Sydney) who kindly provided prostate cancer cell lines. The authors also thank technical support from Mr Ken Hopper, Mr Ese Enari, Mr Alex Wallace, and Mr Peter Treacy from Cancer Care Centre, Sydney, Australia.

#### REFERENCES

1. Beltran H, Beer TM, Carducci MA, de Bono J, Gleave M, Hussain M, Kelly WK, Saad F, Sternberg C, Tagawa ST, Tannock IF. New therapies for castration-resistant prostate cancer: Efficacy and safety. *Eur Urol* 2011;60(2):279–290.
2. Thoms J, Goda JS, Zlotta AR, Fleshner NE, van der Kwast TH, Supiot S, Warde P, Bristow RG. Neoadjuvant radiotherapy for locally advanced and high-risk prostate cancer. *Nat Rev Clin Oncol* 2011;8(2):107–113.
3. Petrylak DP, Tangen CM, Hussain MH, Lara PN Jr, Jones JA, Taplin ME, Burch PA, Berry D, Moynour C, Kohli M, Benson MC, Small EJ, Raghavan D, Crawford ED. Docetaxel and estramustine compared with mitoxantrone and prednisone for advanced refractory prostate cancer. *N Engl J Med* 2004;351(15):1513–1520.
4. Berthold DR, Pond GR, Soban F, de Wit R, Eisenberger M, Tannock IF. Docetaxel plus prednisone or mitoxantrone plus prednisone for advanced prostate cancer: Updated survival in the TAX 327 study. *J Clin Oncol* 2008;26(2):242–245.
5. de Bono JS, Oudard S, Ozguroglu M, Hansen S, Machiels JP, Kocak I, Gravis G, Bodrogi I, Mackenzie MJ, Shen L, Roessner M, Gupta S, Sartor AO, Investigators T. Prednisone plus cabazitaxel or mitoxantrone for metastatic castration-resistant prostate cancer progressing after docetaxel treatment: A randomised open-label trial. *Lancet* 2010;376(9747):1147–1154.
6. Sternberg CN, Dumez H, Van Poppel H, Skoneczna I, Sella A, Daugaard G, Gil T, Graham J, Carpentier P, Calabro F, Collette L, Lacombe D, Group EGTC. Docetaxel plus oblimersen sodium (Bcl-2 antisense oligonucleotide): An EORTC multicenter, randomized phase II study in patients with castration-resistant prostate cancer. *Ann Oncol* 2009;20(7):1264–1269.
7. Nagano O, Okazaki S, Saya H. Redox regulation in stem-like cancer cells by CD44 variant isoforms. *Oncogene* 2013;32(44):5191–5198.
8. Naor D, Sionov RV, Ish-Shalom D. CD44: Structure, function, and association with the malignant process. *Adv Cancer Res* 1997;71:241–319.
9. Hao JL, Ni J, Graham P, Cozzi P, Bucci J, Kearsley J, Li Y. The CD44 isoforms in prostate cancer metastasis and progression. *World J Cancer Res* 2013;1(1):3–14.
10. Khan SA, Cook AC, Kappil M, Gunthert U, Chambers AF, Tuck AB, Denhardt DT. Enhanced cell surface CD44 variant (v6, v9) expression by osteopontin in breast cancer epithelial cells facilitates tumor cell migration: Novel post-transcriptional, post-translational regulation. *Clin Exp Metastasis* 2005;22(8):663–673.
11. Akisik E, Bavbek S, Dalay N. CD44 variant exons in leukemia and lymphoma. *Pathol Oncol Res* 2002;8(1):36–40.
12. Lee JL, Wang MJ, Sudhir PR, Chen GD, Chi CW, Chen JY. Osteopontin promotes integrin activation through outside-in and inside-out mechanisms: OPN-CD44V interaction enhances survival in gastrointestinal cancer cells. *Cancer Res* 2007;67(5):2089–2097.
13. Mulder JW, Wielenga VJ, Polak MM, van den Berg FM, Adolf GR, Herrlich P, Pals ST, Offerhaus GJ. Expression of mutant p53 protein and CD44 variant proteins in colorectal tumorigenesis. *Gut* 1995;36(1):76–80.
14. Christofori G. Changing neighbours, changing behaviour: Cell adhesion molecule-mediated signalling during tumour progression. *EMBO J* 2003;22(10):2318–2323.
15. Gotoda T, Matsumura Y, Kondo H, Saitoh D, Shimada Y, Kosuge T, Kanai Y, Kakizoe T. Expression of CD44 variants and its association with survival in pancreatic cancer. *Jpn J Cancer Res* 1998;89(10):1033–1040.

16. Mulder JW, Kruyt PM, Sewnath M, Oosting J, Seldenrijk CA, Weidema WF, Offerhaus GJ, Pals ST. Colorectal cancer prognosis and expression of exon-v6-containing CD44 proteins. *Lancet* 1994;344(8935):1470–1472.
17. Lipponen P, Aaltoma S, Kosma VM, Ala-Opas M, Eskelinen M. Expression of CD44 standard and variant-v6 proteins in transitional cell bladder tumours and their relation to prognosis during a long-term follow-up. *J Pathol* 1998;186(2):157–164.
18. Ayhan A, Tok EC, Bildirici I, Ayhan A. Overexpression of CD44 variant 6 in human endometrial cancer and its prognostic significance. *Gynecol Oncol* 2001;80(3):355–358.
19. Chen H, Hao J, Wang L, Li Y. Coexpression of invasive markers (uPA, CD44) and multiple drug-resistance proteins (MDR1, MRP2) is correlated with epithelial ovarian cancer progression. *Br J Cancer* 2009;101(3):432–440.
20. Wang L, Chen H, Pourgholami MH, Beretov J, Hao J, Chao H, Perkins AC, Kearsley JH, Li Y. Anti-MUC1 monoclonal antibody (C595) and docetaxel markedly reduce tumor burden and ascites, and prolong survival in an in vivo ovarian cancer model. *PLoS ONE* 2011;6(9):e24405.
21. Hao J, Chen H, Madigan MC, Cozzi PJ, Beretov J, Xiao W, Delprado WJ, Russell PJ, Li Y. Co-expression of CD147 (EMM-PRIN), CD44v3-10, MDR1 and monocarboxylate transporters is associated with prostate cancer drug resistance and progression. *Br J Cancer* 2010;103(7):1008–1018.
22. Xiao W, Graham PH, Power CA, Hao J, Kearsley JH, Li Y. CD44 is a biomarker associated with human prostate cancer radiation sensitivity. *Clin Exp Metastasis* 2012;29(1):1–9.
23. Wang L, Chen H, Liu F, Madigan MC, Power CA, Hao J, Patterson KI, Pourgholami MH, O'Brien PM, Perkins AC, Li Y. Monoclonal antibody targeting MUC1 and increasing sensitivity to docetaxel as a novel strategy in treating human epithelial ovarian cancer. *Cancer Lett* 2011;300(2):122–133.
24. Hao J, Madigan MC, Khatri A, Power CA, Hung TT, Beretov J, Chang L, Xiao W, Cozzi PJ, Graham PH, Kearsley JH, Li Y. In vitro and in vivo prostate cancer metastasis and chemoresistance can be modulated by expression of either CD44 or CD147. *PLoS ONE* 2012;7(8):e40716.
25. Cozzi PJ, Wang J, Delprado W, Perkins AC, Allen BJ, Russell PJ, Li Y. MUC1, MUC2, MUC4, MUC5AC and MUC6 expression in the progression of prostate cancer. *Clin Exp Metastasis* 2005;22(7):565–573.
26. Singh SK, Clarke ID, Terasaki M, Bonn VE, Hawkins C, Squire J, Dirks PB. Identification of a cancer stem cell in human brain tumors. *Cancer Res* 2003;63(18):5821–5828.
27. De Marzo AM, Bradshaw C, Sauvageot J, Epstein JI, Miller GJ. CD44 and CD44v6 downregulation in clinical prostatic carcinoma: Relation to Gleason grade and cytoarchitecture. *Prostate* 1998;34(3):162–168.
28. Gao AC, Lou W, Dong JT, Isaacs JT. CD44 is a metastasis suppressor gene for prostatic cancer located on human chromosome 11p13. *Cancer Res* 1997;57(5):846–849.
29. Noordzij MA, van Steenbrugge GJ, Verkaik NS, Schroder FH, van der Kwast TH. The prognostic value of CD44 isoforms in prostate cancer patients treated by radical prostatectomy. *Clin Cancer Res* 1997;3(5):805–815.
30. Aaltomaa S, Lipponen P, Ala-Opas M, Kosma VM. Expression and prognostic value of CD44 standard and variant v3 and v6 isoforms in prostate cancer. *Eur Urol* 2001;39(2):138–144.
31. Ekici S, Cerwinka WH, Duncan R, Gomez P, Civantos F, Soloway MS, Lokeshwar VB. Comparison of the prognostic potential of hyaluronic acid, hyaluronidase (HYAL-1), CD44v6 and microvessel density for prostate cancer. *Int J Cancer* 2004;112(1):121–129.
32. Takahashi S, Kimoto N, Orita S, Cui L, Sakakibara M, Shirai T. Relationship between CD44 expression and differentiation of human prostate adenocarcinomas. *Cancer Lett* 1998;129(1):97–102.
33. Liotta LA, Delisi C, Sidel G, Kleinerman J. Micrometastases formation: A probabilistic model. *Cancer Lett* 1977;3(3–4):203–208.
34. Ween MP, Oehler MK, Ricciardelli C. Role of Versican, Hyaluronan and CD44 in ovarian cancer metastasis. *Int J Mol Sci* 2011;12(2):1009–1029.
35. Yu Q, Stamenkovic I. Localization of matrix metalloproteinase 9 to the cell surface provides a mechanism for CD44-mediated tumor invasion. *Genes Dev* 1999;13(1):35–48.
36. Sethi S, Macoska J, Chen W, Sarkar FH. Molecular signature of epithelial-mesenchymal transition (EMT) in human prostate cancer bone metastasis. *Am J Transl Res* 2010;3(1):90–99.
37. Mulholland DJ, Kobayashi N, Ruscetti M, Zhi A, Tran LM, Huang J, Gleave M, Wu H. Pten loss and RAS/MAPK activation cooperate to promote EMT and metastasis initiated from prostate cancer stem/progenitor cells. *Cancer Res* 2012;72(7):1878–1889.
38. Kalluri R, Weinberg RA. The basics of epithelial-mesenchymal transition. *J Clin Invest* 2009;119(6):1420–1428.
39. Brown RL, Reinke LM, Damerow MS, Perez D, Chodosh LA, Yang J, Cheng C. CD44 splice isoform switching in human and mouse epithelium is essential for epithelial-mesenchymal transition and breast cancer progression. *J Clin Invest* 2011;121(3):1064–1074.
40. Li C, Heidt DG, Dalerba P, Burant CF, Zhang L, Adsay V, Wicha M, Clarke MF, Simeone DM. Identification of pancreatic cancer stem cells. *Cancer Res* 2007;67(3):1030–1037.
41. Al-Hajj M, Wicha MS, Benito-Hernandez A, Morrison SJ, Clarke MF. Prospective identification of tumorigenic breast cancer cells. *Proc Natl Acad Sci U S A* 2003;100(7):3983–3988.
42. Joshua B, Kaplan MJ, Doweck I, Pai R, Weissman IL, Prince ME, Ailles LE. Frequency of cells expressing CD44, a head and neck cancer stem cell marker: Correlation with tumor aggressiveness. *Head Neck* 2012;34(1):42–49.
43. Yang YM, Chang JW. Bladder cancer initiating cells (BCICs) are among EMA-CD44v6+ subset: Novel methods for isolating undetermined cancer stem (initiating) cells. *Cancer Invest* 2008;26(7):725–733.
44. Hebbard L, Steffen A, Zawadzki V, Fieber C, Howells N, Moll J, Ponta H, Hofmann M, Sleeman J. CD44 expression and regulation during mammary gland development and function. *J Cell Sci* 2000;113(Pt 14):2619–2630.
45. Jijiwa M, Demir H, Gupta S, Leung C, Joshi K, Orozco N, Huang T, Yildiz VO, Shibahara I, de Jesus JA, Yong WH, Mischel PS, Fernandez S, Kornblum HI, Nakano I. CD44v6 regulates growth of brain tumor stem cells partially through the AKT-mediated pathway. *PLoS ONE* 2011;6(9):e24217.
46. Jung P, Sato T, Merlos-Suarez A, Barriga FM, Iglesias M, Rossell D, Auer H, Gallardo M, Blasco MA, Sancho E, Clevers H, Battle E. Isolation and in vitro expansion of human colonic stem cells. *Nat Med* 2011;17(10):1225–1227.
47. Vermeulen L, Todaro M, de Sousa Mello F, Sprick MR, Kemper K, Perez Alea M, Richel DJ, Stassi G, Medema JP. Single-cell cloning of colon cancer stem cells reveals a multi-lineage

- differentiation capacity. *Proc Natl Acad Sci U S A* 2008;105(36):13427–13432.
48. Ponti D, Costa A, Zaffaroni N, Pratesi G, Petrangolini G, Coradini D, Pilotti S, Pierotti MA, Daidone MG. Isolation and in vitro propagation of tumorigenic breast cancer cells with stem/progenitor cell properties. *Cancer Res* 2005;65(13):5506–5511.
  49. Zhang S, Balch C, Chan MW, Lai HC, Matei D, Schilder JM, Yan PS, Huang TH, Nephew KP. Identification and characterization of ovarian cancer-initiating cells from primary human tumors. *Cancer Res* 2008;68(11):4311–4320.
  50. Shi X, Gipp J, Bushman W. Anchorage-independent culture maintains prostate stem cells. *Dev Biol* 2007;312(1):396–406.
  51. Martin GS. Cell signaling and cancer. *Cancer Cell* 2003;4(3):167–174.
  52. Bitting RL, Armstrong AJ. Targeting the PI3K/Akt/mTOR pathway in castration-resistant prostate cancer. *Endocr Relat Cancer* 2013;20(3):R83–R99.
  53. Zhan JF, Wu LP, Chen LH, Yuan YW, Xie GZ, Sun AM, Liu Y, Chen ZX. Pharmacological inhibition of AKT sensitizes MCF-7 human breast cancer-initiating cells to radiation. *Cell Oncol (Dordr)* 2011;34(5):451–456.
  54. Fresno Vara JA, Casado E, de Castro J, Cejas P, Belda-Iniesta C, Gonzalez-Baron M. PI3K/Akt signalling pathway and cancer. *Cancer Treat Rev* 2004;30(2):193–204.
  55. Martelli AM, Evangelisti C, Follo MY, Ramazzotti G, Fini M, Giardino R, Manzoli L, McCubrey JA, Cocco L. Targeting the phosphatidylinositol 3-kinase/Akt/mammalian target of rapamycin signaling network in cancer stem cells. *Curr Med Chem* 2011;18(18):2715–2726.
  56. Dubrovska A, Kim S, Salomone RJ, Walker JR, Maira SM, Garcia-Echeverria C, Schultz PG, Reddy VA. The role of PTEN/Akt/PI3K signaling in the maintenance and viability of prostate cancer stem-like cell populations. *Proc Natl Acad Sci U S A* 2009;106(1):268–273.
  57. Lim M, Chuong CM, Roy-Burman P. PI3K, Erk signaling in BMP7-induced epithelial-mesenchymal transition (EMT) of PC-3 prostate cancer cells in 2- and 3-dimensional cultures. *Horm Cancer* 2011;2(5):298–309.
  58. Pfeil K, Eder IE, Putz T, Ramoner R, Culig Z, Ueberall F, Bartsch G, Klocker H. Long-term androgen-ablation causes increased resistance to PI3K/Akt pathway inhibition in prostate cancer cells. *Prostate* 2004;58(3):259–268.
  59. Dihlmann S, von Knebel Doeberitz M. Wnt/beta-catenin-pathway as a molecular target for future anti-cancer therapeutics. *Int J Cancer* 2005;113(4):515–524.
  60. Du Q, Park KS, Guo Z, He P, Nagashima M, Shao L, Sahai R, Geller DA, Hussain SP. Regulation of human nitric oxide synthase 2 expression by Wnt beta-catenin signaling. *Cancer Res* 2006;66(14):7024–7031.
  61. Sell S. Stem cell origin of cancer and differentiation therapy. *Crit Rev Oncol Hematol* 2004;51(1):1–28.
  62. Yuan D, Liu L, Gu D. Transcriptional regulation of livin by beta-catenin/TCF signaling in human lung cancer cell lines. *Mol Cell Biochem* 2007;306(1–2):171–178.
  63. Seiter S, Arch R, Reber S, Komitowski D, Hofmann M, Ponta H, Herrlich P, Matzku S, Zoller M. Prevention of tumor metastasis formation by anti-variant CD44. *J Exp Med* 1993;177(2):443–455.
  64. Stroemer JW, Roos JC, Sproll M, Quak JJ, Heider KH, Wilhelm BJ, Castelijns JA, Meyer R, Kwakkelstein MO, Snow GB, Adolf GR, van Dongen GA. Safety and biodistribution of 99mTechnetium-labeled anti-CD44v6 monoclonal antibody BIWA 1 in head and neck cancer patients. *Clin Cancer Res* 2000;6(8):3046–3055.
  65. Misra S, Hascall VC, De Giovanni C, Markwald RR, Ghatak S. Delivery of CD44 shRNA/nanoparticles within cancer cells: Perturbation of hyaluronan/CD44v6 interactions and reduction in adenoma growth in Apc Min/+ MICE. *J Biol Chem* 2009;284(18):12432–12446.
  66. Qian C, Wang Y, Chen Y, Zeng L, Zhang Q, Shuai X, Huang K. Suppression of pancreatic tumor growth by targeted arsenic delivery with anti-CD44v6 single chain antibody conjugated nanoparticles. *Biomaterials* 2013;34(26):6175–6184.

## SUPPORTING INFORMATION

Additional supporting information may be found in the online version of this article at the publisher's web-site.